AD669468

[redacted]

DDC
MAY 24 1968
C

PHILCO

PHILCO-FORD CORPORATION
Aeronutronic Division
Newport Beach, California

Best Available Copy

This document has been approved for public release and sale; its distribution is unlimited.

Reproduced by the
CLEARINGHOUSE
for Federal Scientific & Technical
Information Springfield Va. 22151

34

Publication No. U-4132

SCIENTIFIC REPORT

ABSORPTION BY CO_2 BETWEEN 3100 AND 4100 cm^{-1}

(2.44 - 3.22 Microns)

Prepared for: Advanced Research Projects Agency
Washington, D. C.

Under Contract: NOnr 3560(00)
ARPA Order No. 237
Amendment No. 26/9-1-67

Prepared by: Darrell E. Burch
David A. Gryvnak
Richard R. Patty

Approved: Paul M. Sutton
Paul M. Sutton, Manager
Physics Laboratory

30 April 1968

PHILCO Ford
PHILCO-FORD CORPORATION
Aeronutronic Division
Newport Beach, Calif. • 92663

ABSTRACT

The absorption by CO_2 between 3100 and 4100 cm^{-1} has been studied with a spectrometer whose spectral slitwidth was approximately one-half cm^{-1}. Spectral curves were obtained for 26 samples of CO_2 and $CO_2 + N_2$ with pressures as high as 14.6 atmospheres and with paths as long as 933 meters. Several absorption bands not observed previously in laboratory spectra have been identified and the strengths of several bands have been determined. Absorption between 3770 and 4100 cm^{-1} by the extreme wings of strong lines at lower wavenumbers has been investigated for self-broadened and N_2-broadened lines. Spectral curves and extensive tables of $\int_{\nu'}^{\nu} A(\nu)d\nu$ have been included for most of the samples.

TABLE OF CONTENTS

SECTION		PAGE
1	INTRODUCTION AND SUMMARY.	1-1
2	SAMPLE PARAMETERS AND SPECTRAL CURVES	2-1
	TABLE 2-1 - SAMPLE PARAMETERS	2-2
	TABLE 2-2 - SPECTRAL SLITWIDTHS	2-4
	TABLE 2-3 - CO_2 BANDS	2-5
	FIGURE 2-1 - CURVES OF TRANSMITTANCE VS WAVENUMBER FOR VARIOUS SAMPLES.	2-8
	FIGURE 2-2 - " " " " "	2-9
	FIGURE 2-3 - " " " " "	2-10
	FIGURE 2-4 - " " " " "	2-11
	FIGURE 2-5 - " " " " "	2-12
3	INTEGRATED ABSORPTANCE AND BAND STRENGTHS	3-1
	TABLE 3-1 - TABLE OF INTEGRATED ABSORPTANCE BETWEEN 3090 AND 3400 cm^{-1}.	3-3
	TABLE 3-2 - TABLE OF INTEGRATED ABSORPTANCE BETWEEN 3400 AND 3764 cm^{-1}.	3-5
	TABLE 3-3 - TABLE OF INTEGRATED ABSORPTANCE BETWEEN 3777.3 AND 4110.0 cm^{-1}.	3-8
	TABLE 3-4 - INTEGRATED ABSORPTION COEFFICIENT	3-9
	TABLE 3-5 - BAND STRENGTHS (T = 296°K).	3-12
4	WING ABSORPTION BETWEEN 3780 AND 4100 cm^{-1}.	4-1
	FIGURE 4-1 - ABSORPTION COEFFICIENT BETWEEN 3770 AND 4100 cm^{-1} DUE TO WINGS OF STRONG CO_2 LINES AT LOWER WAVENUMBERS	4-3
5	REFERENCES.	5-1

SECTION 1

INTRODUCTION AND SUMMARY

Most of the absorption by CO_2 in the 3100-4100 cm^{-1} region is due to the 02^01 and 10^01 bands of $C^{12}O_2^{16}$ with centers at 3612.8 and 3714.3 cm^{-1}, respectively. However, many other difference bands, combination bands, and isotopic bands also occur in this spectral region. These CO_2 bands play a very important part in the emission by flames and rocket plumes and in the transfer of heat through the atmospheres of the earth and other planets.

Several quantitative measurements of the absorption in this region have been made previously with low resolution.[1,2] The present investigation was undertaken to supplement the previous work with data on samples over wider ranges of pressure and absorber thickness and with sufficient resolution to resolve many of the individual lines. An absorption cell with paths as great as 933 meters has enabled us to study samples of very large absorber thickness without using such high pressures that the structure in the spectral curves would be smoothed out. Shorter absorption cells have also made it possible to study samples at pressures up to 15 atmospheres in order to measure the absorption coefficient and to determine band strengths accurately. Absorption in the 3770-4100 cm^{-1} region by the extreme wings of lines whose centers occur at lower wavenumbers has also been studied for pure CO_2 and for $CO_2 + N_2$ mixtures. The gas-handling procedures and the methods of recording and reducing the data have been described previously.[3,4]

The data are presented in figures and tables of integrated absorptance, $\int A(\nu)d\nu$. Tables of transmittance versus wavenumber are available from the authors.

SECTION 2

SAMPLE PARAMETERS AND SPECTRAL CURVES

Table 2-1 contains the parameters of the samples investigated. Included in the table are the sample number; p, the partial pressure of CO_2; P, the total pressure due to CO_2 and N_2; L, the geometrical path length; and u, the absorber thickness, which is given by

$$u(\text{atm cm}_{STP}) = p(\text{atm})\,[1 + 0.005p]\,L(\text{cm})\,273/296. \qquad (2\text{-}1)$$

The quantity 273/296 accounts for the difference in densities at standard temperature (273°K) and at room temperature (296°K) where all the measurements were made. [1 + 0.005p] accounts for the non-linearity in the relationship between CO_2 pressure and density for the pressures used in the present study.

P_e, the equivalent pressure, was determined from the following equation:

$$P_e = Bp + p_{N_2} = (B-1)\,p + P, \qquad (2\text{-}2)$$

where B = 1.3 is the self-broadening coefficient, the ratio of the self-broadening ability for CO_2 to the N_2-broadening ability.[1]

Figures 2-1 through 2-5 show spectral curves for all samples except 20, 21, 22, 23, and 25 which have been omitted since their pressures were high and the structure in the curves was smoothed out. The wavenumber scale in the figures changes slowly, but over small intervals it can be considered linear. The numbers enclosed in rectangles correspond to the sample numbers. The spectral slitwidth used to scan the curves varied as indicated in Table 2-2.

TABLE 2-1

SAMPLE PARAMETERS

Sample No.	p torr	P torr	P_e torr	p atm	P atm	P_e atm
1	1,900	1,900	2,500	2.5	2.5	3.29
2	1,900	1,900	2,500	2.5	2.5	3.29
3	584	584	762	0.768	0.768	1.002
4	175	175	228	0.230	0.230	0.300
5	176	707	760	0.232	0.930	1.008
6	58.4	58.4	75.9	0.0768	0.0768	0.0999
7	17.5	71.0	76.3	0.023	0.0934	0.1003
8	335	660	761	0.441	0.868	1.002
9	5.8	5.8	7.54	0.00763	0.00763	0.00992
10	5.8	76.0	77.7	0.00763	0.100	0.102
11	335	660	761	0.441	0.868	1.002
12	1.75	7.1	7.62	0.0023	0.00934	0.0103
13	1.75	77	77.5	0.0023	0.101	0.102
14	33.5	752	762	0.0441	0.989	1.003
15	0.58	7.4	7.57	0.000763	0.00973	0.00996
16	33.5	752	762	0.0441	0.989	1.003
17	760	760	993	1.000	1.00	1.31
18	190	760	817	0.25	1.00	1.075
19	11,100	11,100	15,500	14.6	14.6	20.4
20	11,100	11,100	15,500	14.6	14.6	20.4
21	335	11,100	11,200	0.441	14.6	14.7
22	335	11,100	11,200	0.441	14.6	14.7
23	33.5	11,100	11,100	0.0441	14.6	14.6
24	11,100	11,100	15,500	14.6	14.6	20.4
25	2,775	11,100	11,200	3.65	14.6	15.8
26	643	11,100	11,300	0.846	14.6	14.9

TABLE 2-1 (Cont.)

SAMPLE PARAMETERS

Sample No.	L Path m	u atm cm STP	Pages on which spectra appear
1	933	218,000	2-8, 2-9, 2-12
2	237	55,000	2-8, 2-9, 2-12
3	237	16,900	2-8, 2-9, 2-12
4	237	5,040	2-9
5	237	5,070	2-9, 2-12
6	237	1,680	2-11
7	237	503	2-11
8	12.37	503	2-10
9	237	167	2-10
10	237	167	2-10
11	4.16	169	2-10
12	237	50.3	2-11
13	237	50.3	2-11
14	12.37	50.3	2-11
15	237	16.7	2-10
16	4.16	16.9	2-10
17	0.0132	1.22	2-10
18	0.0132	0.305	2-11
19	32.9	47,600	2-12
20	4.16	6,010	Not shown
21	12.4	505	Not shown
22	4.16	169	Not shown
23	12.4	50.4	Not shown
24	0.0134	19.4	2-11
25	0.0134	4.59	Not shown
26	0.0134	1.05	2-11

TABLE 2-2

SPECTRAL SLITWIDTHS

Wavenumber (cm^{-1})	Spectral Slitwidth (cm^{-1})
3100	0.45
3600	0.56
4000	0.67

In spite of considerable care which was exercised to remove the H_2O impurity from the CO_2 samples,[3,4] there was still some structure in the original spectral curves due to H_2O absorption lines. This absorption was particularly troublesome between approximately 3740 cm^{-1} and 3900 cm^{-1} where the H_2O lines are strong and very large samples of CO_2 are required to produce significant absorption. In order to account for the H_2O absorption, spectral curves were obtained for samples of $H_2O + N_2$. The absorber thickness of H_2O was adjusted to approximately match that in the CO_2 sample, and the N_2 pressure was adjusted to match the half-widths of the lines. The matching was done by observing H_2O lines which are isolated from CO_2 lines. The original spectral curves were then corrected by comparing them with the $H_2O + N_2$ curves before they were replotted and digitized. In most cases, the corrections are probably sufficiently accurate that remaining errors in transmittance due to H_2O absorption are not more than a few percent.

The portion of the curve for Sample 6 above 3750 cm^{-1} was not scanned and, therefore, does not appear with the remainder of the curve in the middle panel of Fig. 2-4.

Table 2-3 contains a list of the CO_2 bands from which one might expect appreciable absorption in the 3100-4100 cm^{-1} region for the samples included in the present investigation. The first column of the table contains an arbitrary number assigned to each band. The position of the band center, the energy levels involved in the transition, and the isotoptic species are given in the next three columns. The last column provides a reference to the source from which the information was obtained. SWP indicates that the band center was calculated from energy levels tabulated by Stull, Wyatt, and Plass.[5] Positions of the other band centers were obtained directly from the sources indicated. The positions of the band centers are indicated in Figs. 2-1 to 2-5 by the band numbers listed in Table 2-3. The band numbers are not enclosed in rectangles.

TABLE 2-3

CO_2 BANDS

Band No.	Band Center cm^{-1}	Transition[a]	Isotope[b]	Authority[c]
1	3125.19	$06^00\text{-}01^10$	12, 16, 16	SWP
2	3154.65	$06^20\text{-}01^10$	12, 16, 16	SWP
3	3181.45	05^10	12, 16, 16	PTB
4	3255.78	$15^10\text{-}02^00$	12, 16, 16	SWP
5	3274.87	$14^00\text{-}01^10$	12, 16, 16	SWP
6	3289.55	13^10	13, 16, 16	SWP
7	3339.34	13^10	12, 16, 16	PTB
8	3340.33	$14^20\text{-}01^10$	12, 16, 16	SWP
9	3396.64	$22^00\text{-}01^10$	12, 16, 16	SWP
10	3433.65	21^10	13, 16, 16	SWP
11	3465.34	$04^01\text{-}10^00$	12, 16, 16	PTB
12	3473.675	$04^21\text{-}02^20$	13, 16, 16	C
13	3482.197	$04^01\text{-}02^00$	13, 16, 16	C
14	3490.349	02^01	13, 16, 18	C
15	3497.6	$30^00\text{-}01^10$	13, 16, 16	C
16	3498.719	$03^11\text{-}01^10$	13, 16, 16	C
17	3500.54	21^10	12, 16, 16	PTB
18	3517.300	$12^01\text{-}10^00$	13, 16, 16	C
19	3527.705	02^01	13, 16, 16	C
20	3542.60	$05^11\text{-}03^10$	12, 16, 16	PTB
21	3552.824	$04^21\text{-}02^20$	12, 16, 16	C
22	3568.185	$04^01\text{-}02^00$	12, 16, 16	C
23	3571.105	10^01	12, 16, 18	C
24	3580.295	$03^11\text{-}01^10$	12, 16, 16	C
25	3587.510	10^01	13, 16, 18	C

TABLE 2-3 (Cont.)

CO_2 BANDS

Band No.	Band Center cm^{-1}	Transition[a]	Isotope[b]	Authority[c]
26	3589.609	$12^01 \leftarrow 10^00$	12, 16, 16	C
27	3612.810	02^01	12, 16, 16	C
28	3621.264	$20^01 \leftarrow 10^00$	13, 16, 16	C
29	3621.533	$12^01 \leftarrow 02^00$	13, 16, 16	C
30	3632.876	10^01	13, 16, 16	C
31	3639.181	$11^11 \leftarrow 01^10$	13, 16, 16	C
32	3641.530	$12^21 \leftarrow 02^20$	13, 16, 16	C
33	3675.110	02^01	12, 16, 18	C
34	3692.396	$12^01 \leftarrow 02^00$	12, 16, 16	C
35	3711.438	$20^01 \leftarrow 10^00$	12, 16, 16	C
36	3714.757	10^01	12, 16, 16	C
37	3723.208	$11^11 \leftarrow 01^10$	12, 16, 16	C
38	3726.610	$12^21 \leftarrow 02^20$	12, 16, 16	C
39	3814.260	$20^01 \leftarrow 02^00$	12, 16, 16	C
40	3856.72	14^00	12, 16, 18	SWP
41	3980.57	$01^12 \leftarrow 02^20$	12, 16, 16	SWP
42	4005.89	$00^02 \leftarrow 01^10$	12, 16, 16	B
43	4030.28	$01^12 \leftarrow 02^00$	12, 16, 16	SWI
44	3942.3	14^00 (PI)	12, 16, 16	SWP
45	4064.0	22^20 (PI)	12, 16, 16	SWP

(a) The lower energy level is 00^00 unless indicated otherwise.

(b) The numbers denote the isotopes of C, O, and O, respectively.

(c) Authority for position of band center. SWP, Stull, Wyatt, and Plass[5]; C, Courtoy[6]; PTB, Plyler, Tidwell, and Benedict[7]; and B, Benedict.[8]

(PI) denotes pressure-induced band.

Much of the absorption above 3770 cm^{-1}, particularly for samples at higher pressures, is due to the extreme wings of the strong lines whose centers occur at lower wavenumbers. This wing, or "continuum," absorption is discussed in Section 4. A few weak bands also contribute to the absorption in this region, as can be seen in Fig. 2-5. The relative contributions due to the wing absorption and the absorption by the weak bands can be determined by investigating samples at different pressures since the strengths of the weak bands are independent of pressure, while the absorption coefficient due to the wings of the lines is proportional to pressure.

There is a hint of a pressure-induced band near 4064 cm^{-1}, and possibly another near 3942 cm^{-1}, in the curves corresponding to Samples 1 and 19 in Fig. 2-5. The absorption coefficient for pressure-induced bands is also proportional to pressure; therefore, their contribution is difficult to distinguish from the wing absorption. However, the contour of the curve for Sample 19 suggests the presence of something besides the wing absorption near 4060 cm^{-1}. One would not expect the wing absorption to be nearly constant over a 30 cm^{-1} interval, as occurs between 4030 cm^{-1} and 4060 cm^{-1}, then suddenly decrease at higher wavenumbers. The R-branch of the $01^12 \leftarrow 02^00$ band (No. 43) might contribute slightly between 4030 and 4060 cm^{-1}. However, the "extra" absorption seems to be as strong in the high-pressure samples as in the samples at lower pressure and larger absorber thickness. Therefore, some absorption by the 22^00 (No. 45) pressure-induced band seems likely. Although absorption by the 14^00 pressure-induced band (No. 44) centered at 3942.3 cm^{-1} cannot be confirmed, it probably makes a small contribution. Below approximately 3100 cm^{-1}, there is considerable absorption by the larger samples due to the relatively strong 01^11 pressure-induced band centered at 3004 cm^{-1}.

After correcting for H_2O absorption, we were not able to account for some absorption near 3870 cm^{-1} which causes the deviation from a smooth contour in Fig. 2-5. The relative amounts of absorption at different pressures indicated that it was not due to wing absorption or to a pressure-induced band. However, Benedict[8] has recently attributed absorption in this region in unpublished Venus spectra obtained with better resolution by Pierre and Janine Connes to the 14^00 band (No. 40) of $C^{12}O^{16}O^{18}$. According to Stull, Wyatt, and Plass,[5] this band should be centered at 3856.72 cm^{-1}; therefore, the R-branch is probably responsible for the "extra" absorption seen near 3870 cm^{-1} in Fig. 3-5. The P-branch is probably obscured by the rapidly changing wing absorption and the R-branch of the $20^01 \leftarrow 02^00$ band (No. 39). Evidence of the other bands listed in Table 2-3 with SWP as the authority for the band center can be seen in Figs. 2-1 to 2-5. To the knowledge of the authors none of the bands denoted with SWP have been observed previously in the laboratory. However, all of these bands, as well as several even weaker ones, appear in the Venus spectra obtained by Connes and Connes.

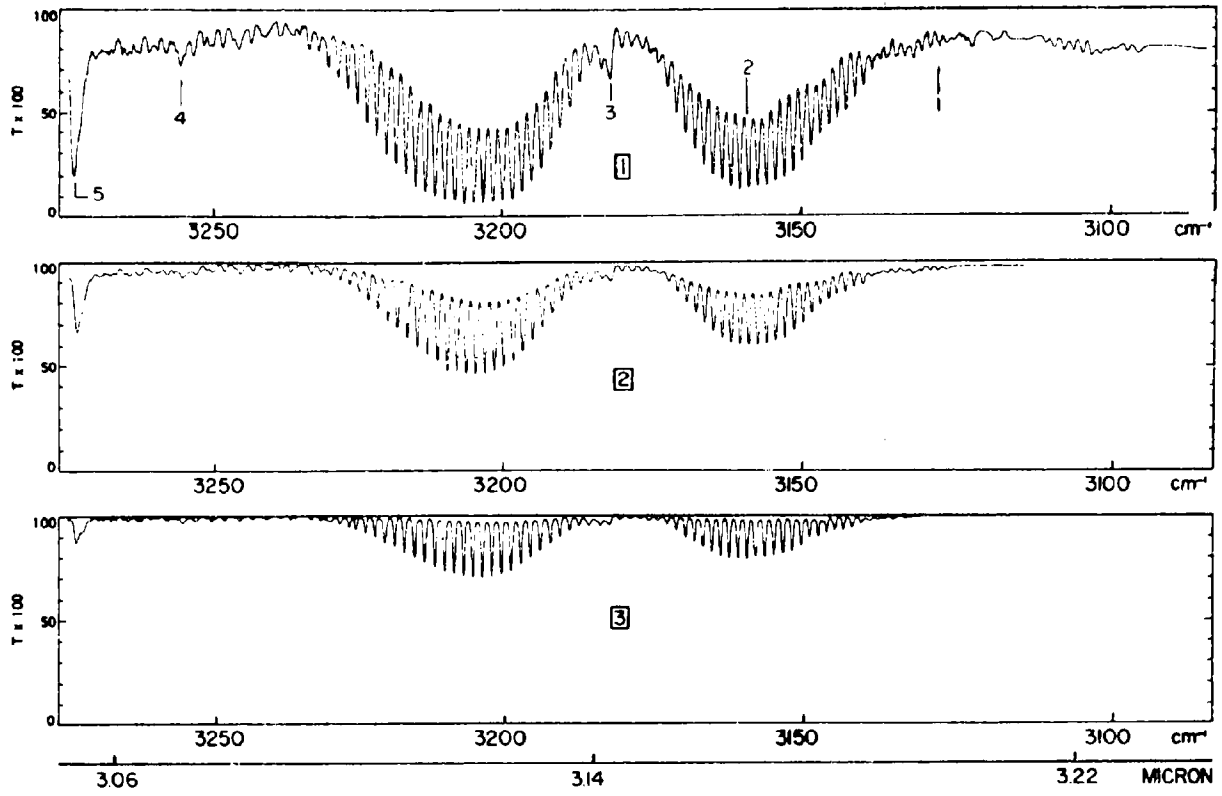

FIG. 2-1. CURVES OF TRANSMITTANCE VERSUS WAVENUMBER FOR VARIOUS SAMPLES.

The sample numbers are enclosed in rectangles. Positions of the band centers are indicated by the number which corresponds to the band number in Table 2-3. Figs. 2-2 through 2-5 are similar but for other spectral regions.

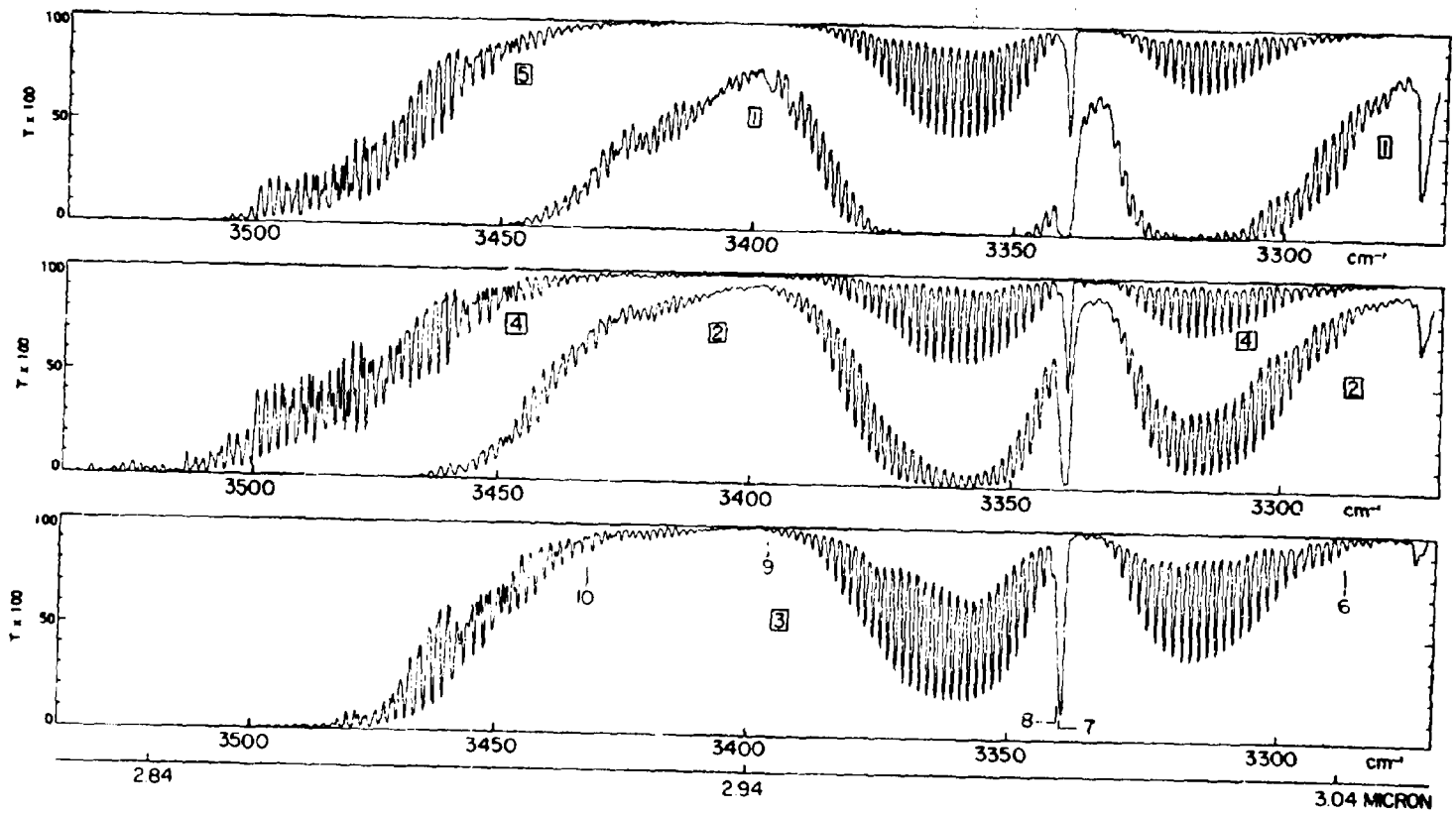
100
50
0
T x 100
5
1
1
3500
3450
3400
3350
3300
cm⁻¹
4
2
4
2
3
9
10
6
8
7
2.84
2.94
3.04 MICRON

Fig. 2-2

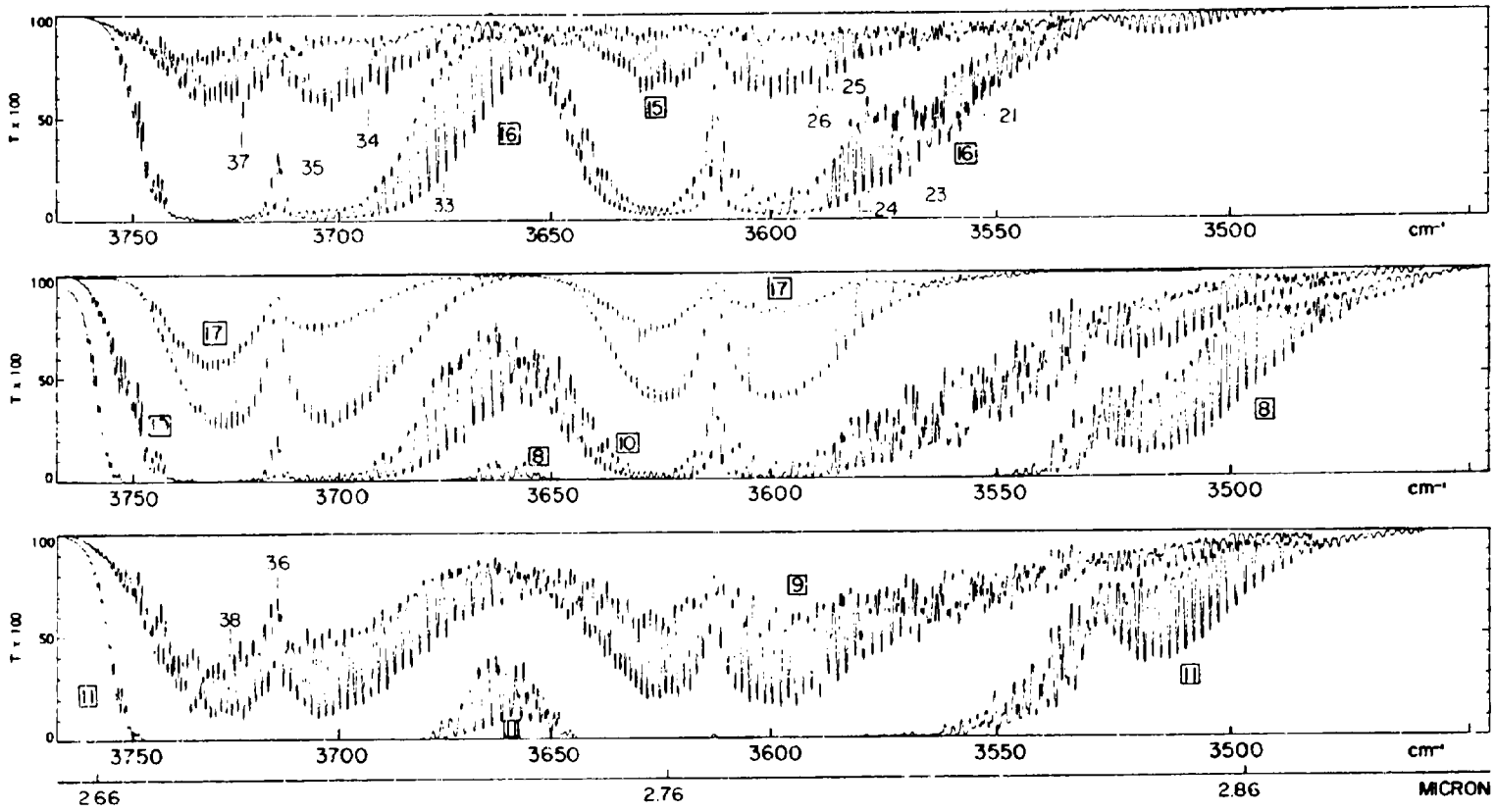
100
50
0
T x 100
37
35
34
33
16
15
25
26
21
16
24
23
3750
3700
3650
3600
3550
3500
cm⁻¹
17
17
15
8
10
8
36
38
9
11
11
11
2.66
2.76
2.86
MICRON

Fig 2-3

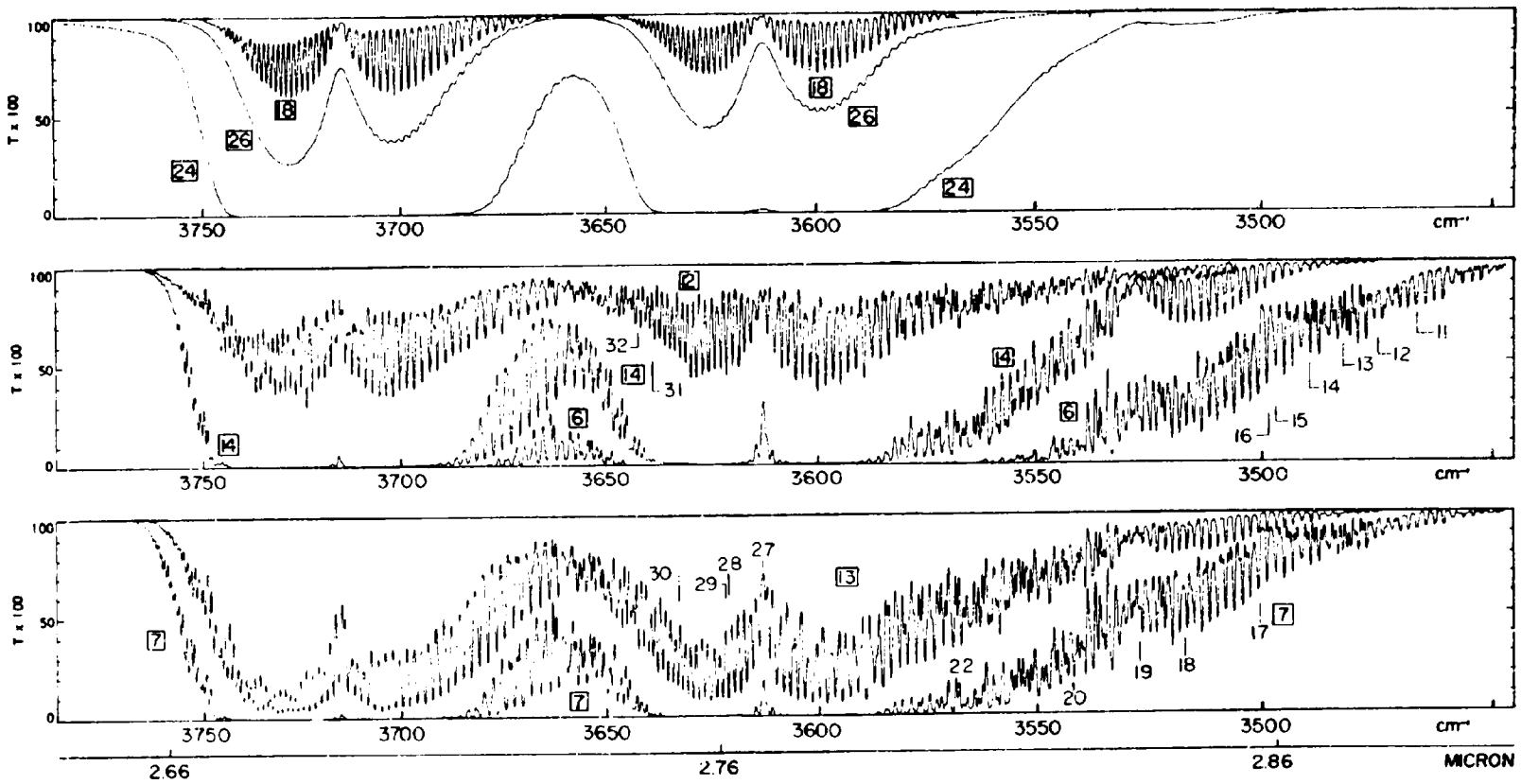
T x 100
100
50
0
3750
3700
3650
3600
3550
3500
cm⁻¹
2.66
2.76
2.86
MICRON
24
26
18
2
14
6
7
13
11
12
15
16
17
19
20
22
27
28
29
30
31
32

Fig. 2-4

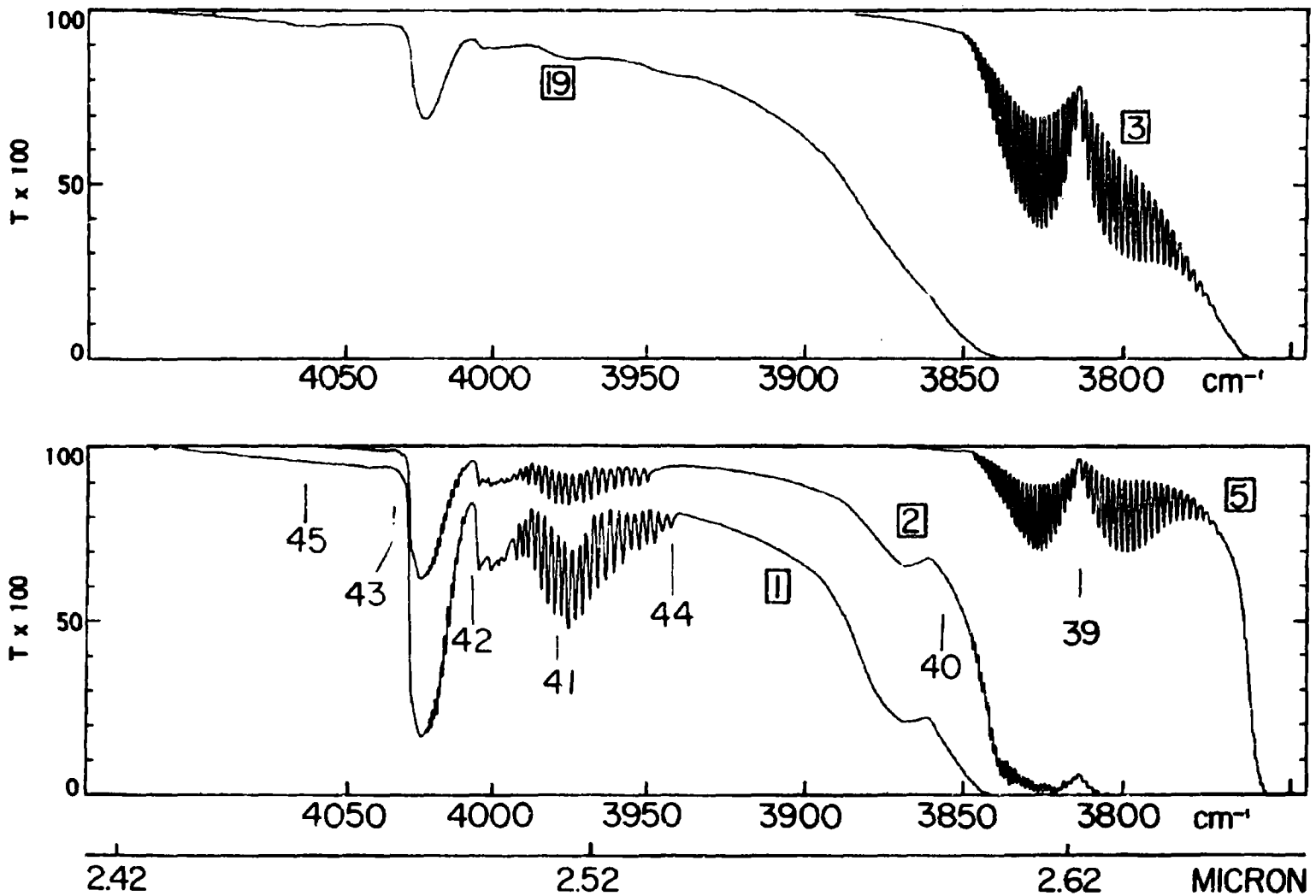
100
50
0
T x 100
19
3
4050
4000
3950
3900
3850
3800
cm⁻¹
100
50
0
T x 100
45
43
42
41
44
1
2
40
39
5
4050
4000
3950
3900
3850
3800
cm⁻¹
2.42
2.52
2.62
MICRON

Fig. 2-5

SECTION 3

INTEGRATED ABSORPTANCE AND BAND STRENGTHS

Tables 3-1 to 3-3 give the integrated absorptance, $\int_{\nu'}^{\nu} A(\nu)d\nu$, for several of the samples investigated. ($A(\nu) \equiv 1-T(\nu)$) Each of the tables covers one of the three following spectral regions: 3090-3400 cm^{-1}, 3400-3764 cm^{-1}, and 3777.3-4100 cm^{-1}. Each column corresponds to the sample whose parameters are given at the top along with ν', the lower limit of integration. In regions where the structure of the curves is regular, the cumulative integral is tabulated at points midway between the centers of the absorption lines. Therefore, if there is no overlapping, the difference between successive tabulated values is the integrated absorptance, or equivalent width, of the absorption line in the interval. In regions where there is little structure, or where it is irregular, the values are tabulated at convenient integral or half-integral wavenumbers. Tables of transmittance versus wavenumber have been compiled but are not included in this report because of their excessive size. However, copies can be obtained from the authors by workers who require them.

The 3400-3764 cm^{-1} region contains the strongest bands, and several of the larger samples are opaque ($A(\nu) = 1$) over wide intervals in this region. In some cases the integrated absorptance tables do not include the opaque regions, which are apparent in Figs. 2-1 to 2-5. The 3090-3400 and 3777.3-4100 cm^{-1} spectral regions contain weaker bands so that only the larger samples produce significant absorption. The intervals for which values have been tabulated for each sample are limited to places where the absorptance is sufficiently large to be measured with reasonable accuracy. In the interval between 3764 and 3777 cm^{-1}, which is not included in the tables, Samples 1, 2, and 19 are opaque. The absorptance in this interval changes rapidly with wavenumber for the smaller samples and is nearly negligible for Samples 9-18.

The cumulative integral, rather than the integral over short intervals, has been tabulated in Tables 3-1 to 3-3 in order that the integrated absorptance over any wavenumber interval listed in the tables can be found quickly by subtracting the values of the integral tabulated at the ends of the interval. The average absorptance over the interval is found by dividing the integrated absorptance by the width of the interval in cm^{-1}.

The true transmittance, $T'(\nu)$, that would be observed with infinite resolving power is related to the absorption coefficient $K(\nu)$ by

$$T'(\nu) = \exp\left[-uK(\nu)\right], \text{ or } K(\nu) = -\frac{1}{u}\ln T'(\nu). \tag{3-1}$$

We have shown in a previous report[9] that if sample pressures are sufficiently high the line structure in a spectrum is smoothed out and $T(\nu)$, the observed transmittance, is approximately equal to $T'(\nu)$. Therefore, under this condition, the absorption coefficient can be determined from transmission spectra by substituting $T(\nu)$ for $T'(\nu)$ in Eq. (3-1). In the case of an isolated band which is not overlapped by a neighboring band, the strength S_ν of the band is given by

$$S_\nu = \int K(\nu)d\nu = -\frac{1}{u}\int \ln T'(\nu)d\nu. \qquad \text{(non-overlapping band)} \tag{3-2}$$

When there is overlapping of two or more bands, the contributions of each to the absorption must be determined before their strengths can be found.

By investigating samples covering very wide ranges of absorber thickness and at pressures up to 14.6 atm, we have determined $-\frac{1}{u}\int \ln T'(\nu)d\nu$ over six spectral regions from 3120 to 3780 cm^{-1}. As can be seen below, these six regions were chosen over intervals which are convenient for determining the strengths of the different branches of several bands. The results are summarized in Table 3-4 which also lists the bands contributing to the absorption in each of the spectral regions. Although relatively high pressures were required to measure $-\frac{1}{u}\int \ln T'(\nu)d\nu$, it should be noted that this quantity is essentially independent of pressure over the regions listed in Table 3-4 if P is less than 4 or 5 atm. However, as mentioned in the previous section, the absorption coefficient on either side of the interval covered in the table increases with pressure, because of the pressure-induced bands and the wing absorption.

Table 3-1 $\int_{\nu} A(\nu)\, d\nu$

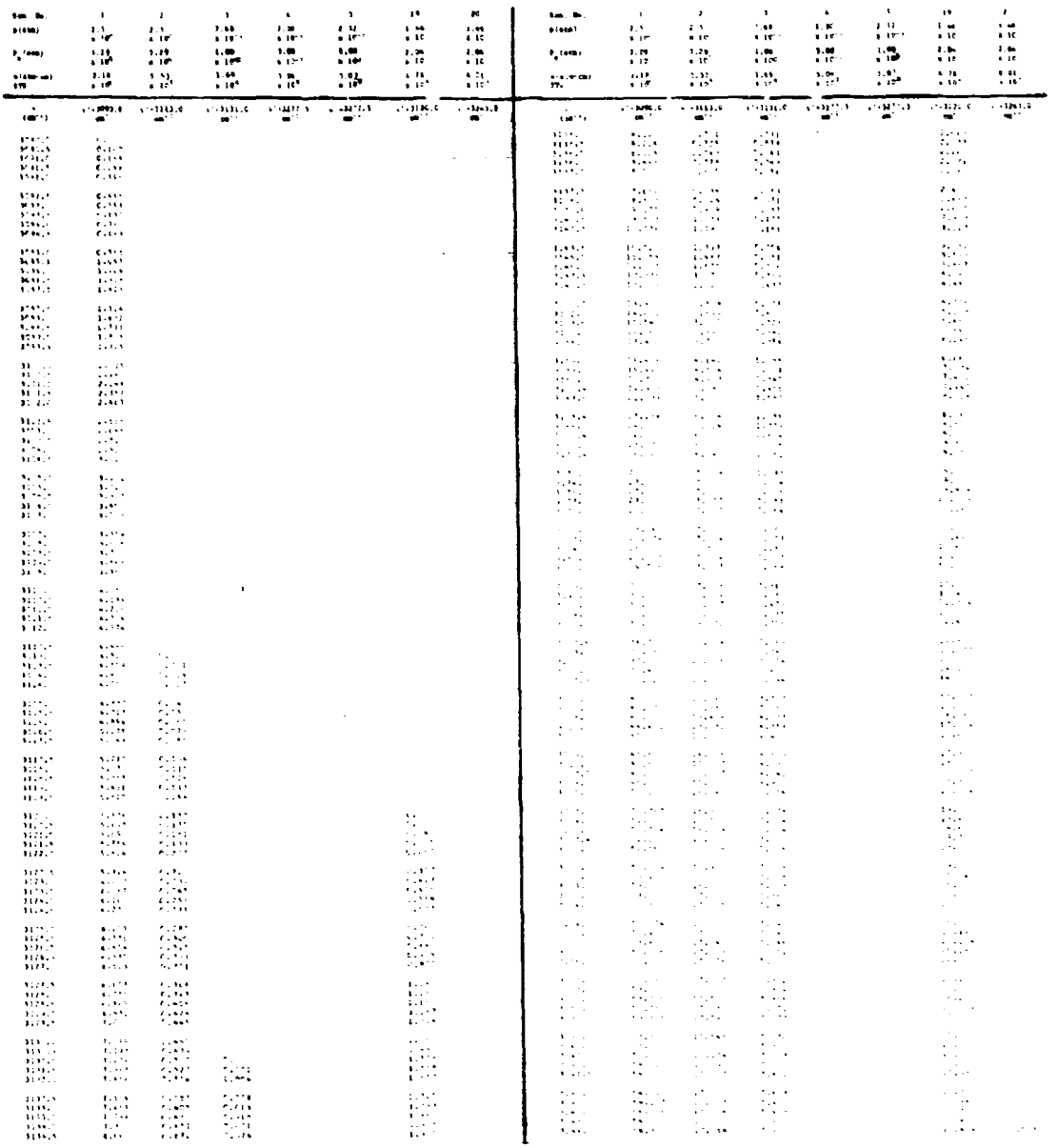

Table 3-1 $\int_{\nu} A(\nu)\,d\nu$ (cont'd)

Table 3-2 $\int_{\nu} \hat{A}(\nu)\, d\nu$

Table 3-2 $\int_{\nu} \bar{A}(\nu)\, d\nu$ (cont'd)

Table 3-2 $\int_{\nu} A(\nu)\,d\nu$ (cont'd)

Table 3-3 $\int_{\nu} A(\nu)\, d\nu$

Sam. No.	1	2	3	5	19
p(atm)	2.5 × 10	2.5 × 10	3.48 × 10⁻¹	2.31 × 10⁻¹	1.46 × 10
P_e(atm)	3.28 × 10⁻	3.75 × 10	1.00 × 100	1.00 × 100	2.04 × 10
u(atm-cm) STP	2.15 × 10⁴	3.53 × 10⁴	1.69 × 10⁴	5.01 × 10⁴	4.76 × 10⁴
ν (cm⁻¹)	ν'=3777.3 cm⁻¹	ν'=3777.3 cm⁻¹	ν'=3777.3 cm⁻¹	ν'=3777.3 cm⁻¹	ν'=3777.3 cm⁻¹
3777.3	0.	0.	0.	0.	0.
3779.5	2.000	2.000	1.569	0.366	2.000
3781.9	4.000	10.000	3.069	0.704	4.000
3783.9	6.000	6.000	4.499	1.025	6.000
3785.2	7.900	7.830	5.874	1.328	7.950
3787.1	9.400	9.400	7.097	1.632	9.800
3789.0	11.700	11.700	8.372	1.944	11.700
3791.6	13.400	13.600	9.556	2.260	13.600
3792.7	15.400	15.400	10.676	2.571	15.400
3794.6	17.300	17.300	11.753	2.963	17.300
3796.4	19.100	19.100	12.436	3.257	19.100
3798.2	20.900	20.900	13.867	3.593	20.900
3800.0	22.700	22.700	14.892	3.935	22.700
3801.7	24.400	24.400	15.894	4.249	24.400
3803.4	26.100	26.100	16.812	4.584	26.100
3805.1	27.800	27.700	17.707	4.884	27.800
3806.8	29.500	29.400	18.594	5.183	29.500
3808.4	31.100	31.000	19.375	5.453	31.100
3810.1	32.800	32.700	20.174	5.862	32.800
3811.7	34.400	34.332	20.906	5.867	34.400
3813.4	36.100	36.149	21.781	5.946	36.100
3815.0	37.700	37.945	22.798	6.072	37.700
3817.1	39.800	39.487	23.296	6.236	39.800
3818.6	41.300	40.990	23.803	6.428	41.300
3820.1	42.800	42.409	24.479	6.671	42.800
3821.5	44.200	43.799	24.395	6.917	44.200
3822.9	45.600	45.108	24.769	7.142	45.600
3824.3	47.000	46.540	25.441	7.446	47.000
3825.7	48.400	47.929	26.397	7.771	48.400
3827.1	49.800	49.747	26.771	8.048	49.700
3828.4	51.100	50.591	27.197	7.162	51.100
3829.7	52.400	51.912	27.971	8.418	52.400
3831.0	53.700	53.067	28.567	8.781	53.700
3832.3	54.900	54.223	29.244	9.110	54.800
3833.	[illegible]	55.456	29.812	9.339	56.100
3834.7	57.400	56.591	30.100	9.510	57.300
3835.9	58.600	57.122	30.535	9.666	58.500
3837.1	59.800	58.033	30.945	9.800	59.700
3838.2	60.900	59.847	31.571	9.925	60.800
3839.4	62.100	60.930	31.882	10.036	62.094
3840.5	63.200	61.881	31.937	10.126	63.173
3841.6	64.200	62.782	32.188	10.264	64.261
3842.6	65.271	63.678	32.619	10.372	65.441
3843.6	66.470	64.592	32.944	10.518	66.419
3844.6	67.337	65.355	32.765	10.565	67.585
3845.6	68.326	66.755	32.879	10.593	68.652
3846.6	69.394	68.374	33.037	10.636	69.561
3847.5	70.311	69.848	33.394	10.693	70.448
3848.5	71.435	67.357	33.147	10.665	71.389
3849.4	72.260	69.312	33.101	10.675	72.264
3850.3	73.791	69.968	33.514	10.629	73.830
3851.2	74.788	71.720	33.314	10.588	74.861
3852.1	75.891	73.161	33.871	10.629	75.920
3853.	76.919	75.039	34.122	10.650	76.958
3853.8	77.952	76.562	34.235	10.678	77.109
3854.7	78.727	77.966	34.370	10.696	78.184
3855.5	79.576	79.033	34.394	10.715	79.985
3856.3	80.843	79.673	34.444	10.720	80.279
3857.1	82.811	81.344	34.571	10.728	82.375
3857.9	83.540	82.936	34.545	10.733	83.765
3858.8	84.829	83.997	34.592	10.736	84.952
3859.5	85.583	85.932	34.611	10.736	85.481
3860.3	86.974	87.314	34.637	10.736	86.893
3861.0	88.225	88.653	34.646	10.736	88.152
3861.8	89.414	89.512	34.652	10.736	89.315
3862.5	90.524	90.346	34.652	10.736	90.341
3863.2	91.576	91.663	34.652	10.736	91.369
3863.8	92.567	92.928	34.652	10.736	92.322
3864.4	93.413	94.277	34.652	10.736	93.342
3865.0	94.525	94.481	34.652	10.736	94.897
3865.7	95.549	96.610	34.652	10.736	95.273
3866.4	96.641	96.465	34.652	10.736	96.654
3867.0	97.284	98.126	34.652	10.736	97.065
3867.6	98.879	99.311	34.652	10.736	97.468
3868.4	99.691	99.537	34.652	10.736	97.826
3869.0	100.641	99.775	34.652	10.736	98.187
3869.7	101.158	98.038	34.652	10.736	98.569
3870.3	101.874	98.236	34.652	10.736	98.897
3870.9	102.613	99.514	34.652	10.736	99.249
3871.6	103.779	99.936	34.652	10.736	99.585
3872.2	104.720	97.088	34.652	10.736	99.957
3872.8	105.517	97.344	34.652	10.736	100.219
3873.4	106.343	97.597	34.652	10.736	100.517
3874.5	107.276	97.814	34.652	10.736	100.785
3875.7	107.717	98.918	34.652	10.736	101.031

Sam. No.	1	2	3	5	19
p(atm)	2.5 × 10⁻	2.5 × 10⁻	3.48 × 10⁻¹	2.31 × 10⁻¹	1.46 × 10
P_e(atm)	3.28 × 10⁻	3.29 × 10⁻	1.00 × 10⁻	1.00 × 10⁻	2.04 × 10
u(atm-cm) STP	2.10 × 10⁴	3.55 × 10⁴	1.69 × 10⁴	3.07 × 10⁴	4.76 × 10⁴
ν (cm⁻¹)	ν'=3777.3 cm⁻¹	ν'=3777.3 cm⁻¹	ν'=3777.3 cm⁻¹	ν'=3777.3 cm⁻¹	ν'=3777.3 cm⁻¹
3987.6	126.247	88.170	34.652	10.736	121.251
3989.4	126.745	88.3.	.652	10.736	121.456
3991.8	129.207	88.46-	652	10.736	121.862
3993.7	127.613	88.55	652	10.736	121.861
3995.6	130.736	88.71	.652	10.736	122.063
3998.0	131.095	89.067	.652	10.736	122.921
4000.3	131.754	89.262	34.652	10.736	122.543
4002.0	132.635	89.451	34.652	10.736	122.718
4.34.7	133.240	88.664	34.652	10.736	122.983
4006.2	133.748	89.946	34.652	10.736	123.192
4008.1	134.130	89.953	34.652	10.736	123.379
4009.8	134.391	90.027	34.652	10.736	123.311
4011.5	134.677	90.113	34.652	10.736	123.641
4013.3	135.031	90.212	34.652	10.736	123.779
4015.0	135.447	90.367	34.652	10.736	123.936
4016.8	135.934	90.501	34.652	10.736	124.113
4018.4	136.547	90.689	34.652	10.736	124.317
4017.1	137.114	90.924	34.652	10.736	124.533
4019.2	137.805	91.155	34.652	10.736	124.762
4019.2	138.484	91.422	34.652	10.736	125.039
4020.2	139.222	91.715	34.652	10.736	125.361
4021.1	139.926	92.031	34.652	10.736	125.562
4022.0	140.611	92.305	34.652	10.736	125.836
4022.8	141.292	92.569	34.652	10.736	126.083
4023.6	141.913	92.860	34.652	10.736	126.333
4024.3	142.475	93.145	34.652	10.736	126.555
4025.0	142.935	93.364	34.652	10.736	126.731
4025.5	143.472	93.591	34.652	10.736	126.916
4026.1	143.943	93.811	34.652	10.736	127.072
4026.7	144.544	93.866	34.652	10.736	127.049
4027.4	144.276	93.917	34.652	10.736	127.151
4028.0	144.345	93.986	34.652	10.736	127.201
4028.5	144.523	94.055	34.652	10.736	127.291
4029.0	144.587	94.127	34.652	10.736	127.290
4029.7	144.915	94.141	34.652	10.736	127.344
4027.4	144.988	94.237	34.652	10.736	127.387
4027.0	145.139	94.315	34.652	10.736	127.427
4028.8	145.250	94.377	34.652	10.736	127.464
4029.0	145.437	94.417	34.652	10.736	127.497
4029.7	145.565	94.497	34.652	10.736	127.526
4029.4	145.726	94.534	34.652	10.736	127.551
4029.6	145.862	94.628	34.652	10.736	127.575
4029.8	145.982	94.654	34.652	10.736	127.591
4030.0	146.294	94.753	34.652	10.736	127.695
4030.2	146.317	94.761	34.652	10.736	127.720
4030.4	146.318	94.763	34.652	10.736	127.721
4030.6	146.358	94.772	34.652	10.736	127.734
4030.8	146.373	94.777	34.652	10.736	127.746
4031.0	146.389	94.782	34.652	10.736	127.758
4031.2	146.417	94.787	34.652	10.736	127.777
4031.4	146.435	94.792	34.652	10.736	127.779
4031.6	146.453	94.797	34.652	10.736	127.793
4031.8	146.475	94.931	34.652	10.736	127.803
4032.0	146.486	94.845	34.652	10.736	127.811
4032.2	146.502	94.9	34.652	10.736	127.823
4032.4	146.518	94.812	34.652	10.736	127.832
4032.6	146.533	94.816	34.652	10.736	127.842
4032.8	146.547	94.819	34.652	10.736	127.852
4033.0	146.561	94.822	34.652	10.736	127.862
4033.2	146.575	94.825	34.652	10.736	127.869
4033.4	146.585	94.828	34.652	10.736	127.879
4033.6	146.602	94.832	34.652	10.736	127.888
4033.8	146.616	94.832	34.652	10.736	127.899
4034.0	146.628	94.835	34.652	10.736	127.907
4034.2	146.644	94.847	34.652	10.736	127.953
4040.0	146.963	94.919	34.652	10.736	128.165
4045.0	147.299	94.985	34.652	10.736	128.376
4050.3	147.584	95.045	34.652	10.736	128.537
4055.0	147.866	95.098	34.652	10.736	128.812
4060.0	148.069	95.149	34.652	10.736	129.039
4065.0	148.316	95.146	34.652	10.736	129.276
4070.0	148.557	95.216	34.652	10.736	129.458
4075.0	148.748	95.242	34.652	10.736	129.672
4080.0	148.926	95.266	34.652	10.736	129.862
4085.0	149.095	95.272	34.652	10.736	129.973
4090.0	149.258	95.277	34.652	10.736	130.097
4095.0	149.335	95.277	34.652	10.736	130.197
4100.0	149.425	95.277	34.652	10.736	130.276
4105.0	149.510	95.277	34.652	10.736	130.291
4110.0	149.539	95.277	34.652	10.736	130.317

TABLE 3-4

INTEGRATED ABSORPTION COEFFICIENT

Spectral Region (cm^{-1})	$-\frac{1}{u}\int \ln T'(\nu)d\nu$ ($atm^{-1} cm^{-1}_{STP} cm^{-1}$)	Contributing Bands
3120.0 - 3249.0	3.8×10^{-4}	1, 2, 3
3249.0 - 3280.0	4.4×10^{-5}	4, 5, 6
3280.0 - 3400.0	3.2×10^{-3}	6 - 9
3400.0 - 3470.0	3.3×10^{-3}	9 - 13
3470.0 - 3658.3	32.4	12 - 32
3658.3 - 3780.0	47.7	32 - 38

The major sources of error in measurements of $(-1/u)\int \ln T'(\nu)d\nu$ are:

(i) errors in sampling which produce errors in the value of u,
(ii) errors caused by differences between $T'(\nu)$ and $T(\nu)$ which arise because the lines are not sufficiently broadened, or the spectral slitwidth is too great, and
(iii) errors in placing the zero-absorptance curve on the sample curve.

Errors due to (i) are probably less than one percent when pure CO_2 samples are used. However, this type of error may be as large as 2 or 3 percent in Samples 25 and 26, which were used from approximately 3570 to 3640 cm^{-1} and from 3675 to 3750 cm^{-1}. The additional uncertainty in these samples arises from pre-mixing the CO_2 and N_2 before introducing the mixture into the 1.34 cm cell. Errors due to (ii) are usually less than 1 or 2 percent if the samples are at approximately 14.6 atm and the transmittance is not too low. We[9] have discussed previously the dependence of this type of error on line width, line spacing, and transmittance. In order to minimize this type of error, we restricted the samples used in a given spectral region to those whose transmittances were greater than approximately 0.2.

Errors of type (iii) are probably the most serious, particularly in regions where the absorptance is small. Wherever possible, we used samples only in regions where the absorptance was greater than approximately 0.2 in order to minimize this error. This was not possible in the narrow regions of weak absorption near 3120 cm^{-1} and 3250 cm^{-1} where even the largest 14.6 atm sample (19) produced less than 0.2 absorptance. The total estimated uncertainties for the values in Table 3-4 are $\pm$ 8% for the 3120.0-3249.0 cm^{-1} region and $\pm$ 5% for the other regions.

The value 32.4 $\pm$ 5% atm^{-1} cm^{-1}_{STP} cm^{-1} for the 3470-3658.3 cm^{-1} region agrees favorably with 37 $\pm$ 20% obtained by Burch, Gryvnak, and Williams[1] and 27.3 $\pm$ 10% by Eggers and Crawford.[10] The latter two values were obtained with instruments having considerably lower resolving power and with samples at lower pressures so that the required corrections for the effect of the finite slit width were greater. Therefore, the present value is regarded as more reliable. The same comments apply to a similar comparison of the 47.7 $\pm$ 5% atm^{-1} cm^{-1}_{STP} cm^{-1} obtained for the 3658.3-3780.0 cm^{-1} region. Burch, Gryvnak, and Williams[1] reported 54 $\pm$ 20%, while Eggers and Crawford[10] obtained 39.1 $\pm$ 10% in the same units.

Although several bands contribute to the absorption in each of the optical regions listed in Table 3-4, four of the six regions contain one band which gives rise to most of the absorption. By following the procedure described previously[11] to account for the overlapping bands, difference bands, and isotopic bands, we have been able to determine the strengths of each branch of the major bands (3, 7, 27, and 36) in these four regions. The strength, S_Q, of the prominent Q branch of Band No. 5 was also determined, although overlapping by lines of other bands made it impractical to attempt to determine the strengths of the P and R branches. The strengths of these bands are given in Table 3-5 along with the strengths of Bands 39 and 42 (S_ν denotes the strength of an entire band). The uncertainties in the strengths of Bands 3, 7, 27, and 36 are only slightly greater than the uncertainties in the corresponding values of integrated absorption coefficient listed in Table 3-4 since the corrections made for overlapping bands are relatively small. Overlapping by the continuum due to the wings of the strong lines at lower wavenumbers also had to be accounted for in order to determine the strengths of Bands 39 and 42. Since the continuum was quite significant at high pressures, the strengths could not be determined as accurately as for the other bands listed in Table 3-5.

Plyler, Tidwell, and Benedict[7] have measured the strengths of Bands 3 and 7 and have determined from lines P72-74 the strength of Band 27. We have modified their results to account for the difference between the density of CO_2 at 273°K and at 298°K, and the temperature of their samples, so that we can compare them with our values given in atm^{-1} cm^{-1}_{STP} cm^{-1}. These results are also given in Table 3-5. Although Plyler et al have

stated that their techniques were not designed to yield strength measurements of high precision, their results are in fair-to-good agreement with ours. The principal uncertainty in the measurements of Plyler et al arose from the presence of atmospheric H_2O lines and from the noise level. These sources of errors were greatly reduced in the present investigation since the optical path outside the absorption cell was evacuated and the larger sample produced absorption which was much greater than the noise. Abnormalities in the distribution of the strengths within the P, Q, and R branches of several bands in this spectral region have been discussed by Plyler et al.

TABLE 3-5

BAND STRENGTHS (T = 296°K)

Band No.	Band Center (cm^{-1})	Transition	Strengths ($atm^{-1} cm^{-1}_{STP} cm^{-1}$)		
			Present Results		Plyler et al*
3	3181.45	$05^{1}0$	S_P	$1.1 \times 10^{-4} \pm 10\%$	
			S_{R+Q}	$2.4 \times 10^{-4} \pm 8\%$	
			S_V	$3.5 \times 10^{-4} \pm 8\%$	$3.6 \times 10^{-4} \pm 10\%$
5	3274.87	$14^{0}0 \leftarrow 01^{1}0$	S_Q	$1.9 \times 10^{-5} \pm 20\%$	
7	3339.34	$13^{1}0$	S_P	$7.0 \times 10^{-4} \pm 6\%$	
			S_Q	$2.1 \times 10^{-4} \pm 10\%$	
			S_R	$2.0 \times 10^{-3} \pm 6\%$	
			S_V	$2.9 \times 10^{-3} \pm 6\%$	$3.8 \times 10^{-4} \pm 10\%$
27	3612.81	$02^{0}1$	S_P	$13.8 \pm 6\%$	
			S_R	$15.2 \pm 6\%$	
			S_V	$29.0 \pm 6\%$	$33 \pm 10\%$
36	3714.76	$10^{0}1$	S_P	$21.3 \pm 6\%$	
			S_R	$23.6 \pm 6\%$	
			S_V	$44.9 \pm 6\%$	
39	3814.26	$20^{0}1 \leftarrow 02^{0}0$	S_P	$9.1 \times 10^{-4} \pm 20\%$	
			S_R	$10.5 \times 10^{-4} \pm 20\%$	
			S_V	$19.6 \times 10^{-4} \pm 20\%$	
42	4005.89	$00^{0}2 \leftarrow 01^{1}0$	S_{P+Q}	5.4×10^{-5} + 15% - 5%	
			S_R	9.5×10^{-5} + 10% - 2%	
			S_V	14.9×10^{-5} + 12% - 3%	

*Plyler, Tidwell, and Benedict[7]

SECTION 4

WING ABSORPTION BETWEEN 3780 AND 4100 cm^{-1}

The contribution to the absorption between 3780 and 4100 cm^{-1} by the lines occurring in the region can be estimated and subtracted from the observed absorption to obtain the contribution by the extreme wings of the strong lines whose centers occur at lower wavenumbers. The following discussion refers only to the absorption by the extreme wings, which is frequently called continuum absorption because of the lack of structure in the spectrum.

It is well known that the absorption coefficient of a single, collision-broadened absorption line is proportional to pressure at any point more than a few half-widths from the line center. Therefore, since the continuum absorption between 3780 and 4100 cm^{-1} is due to the sum of the wing contributions of many lines, we expect the absorption coefficient to be proportional to pressure. We[12] have previously demonstrated this to be true for continuum absorption above the head of the 1.4 μ (00^03) CO_2 band.

For a sample of pure CO_2, when there is self-broadening only, the absorption coefficient is given by

$$K_s(\nu) = K_s^o(\nu)p/p^o, \qquad (4\text{-}1)$$

where the subscript s refers to self-broadening and the superscript o indicates a pressure of 1 atm. Since there is no structure in the continuum absorption and it does not change appreciably over an interval equal to our spectral slitwidth, we assumed that the observed transmittance was equal to the true transmittance $T'(\nu)$. Therefore, we were able to determine the absorption coefficient for the continuum from the spectral

curves, after accounting for the nearby lines, by the use of Eq. (3-2). By combining this equation with Eq. (4-1), we get for a pure CO_2 sample,

$$K_s^o(\nu) = -\frac{p^o}{up} \ln T(\nu). \tag{4-2}$$

In the case of a mixture of CO_2 plus a non-absorbing foreign gas with partial pressure p_f, the absorption coefficient results from the sum of the self-broadening and the foreign-broadening and is given by

$$K(\nu) = K_s(\nu) + K_f(\nu). \tag{4-3}$$

Since K_f is proportional to p_f, we can write

$$-\frac{1}{u} \ln T(\nu) = K_s^o(\nu)p/p^o + K_f^o(\nu)p_f/p^o. \tag{4-4}$$

From curves of transmittance for pure samples covering wide ranges of pressure and path length, we have determined $K_s^o(\nu)$ at several points where the contribution by nearby lines is small. The results are shown in Fig. 4-1, along with similar results for N_2 broadening. The latter results were obtained from curves for $CO_2 + N_2$ mixtures by the use of Eq. (4-4) after K_s^o had been determined. Most of the points are based on samples at pressures from approximately 7 to 15 atm, since the relative contribution of the nearby lines is less at high pressures. The greatest uncertainty in the results is due to errors in accounting for the nearby lines. The estimated uncertainty in the curves of Fig. 4-1 is approximately $\pm$ 10% for $\nu < 3900$ cm^{-1}; at higher wavenumbers, it increases to approximately $\pm$ 30% at 4100 cm^{-1}.

It is of interest to note that $K_{N_2}^o$ is only about 0.1 times as great as K_s^o near 3780 cm^{-1}, but it is nearly 0.5 times as great near 3900 cm^{-1}. We[13] have shown previously that the absorption coefficient at about 1 cm^{-1} from the center of an N_2-broadened line is approximately 0.8 times as great as that for an equally-strong, self-broadened line when the pressures are equal. Therefore, since $K_{N_2}^o/K_s^o$ is as small as 0.1 at a point where most of the absorption is due to distant lines, we can conclude that the shapes of the wings of self-broadened and N_2-broadened lines are quite different. A separate report[14] dealing with the shapes of the wings of lines in this region and in the 1.4 and 4.3 μ regions is being written.

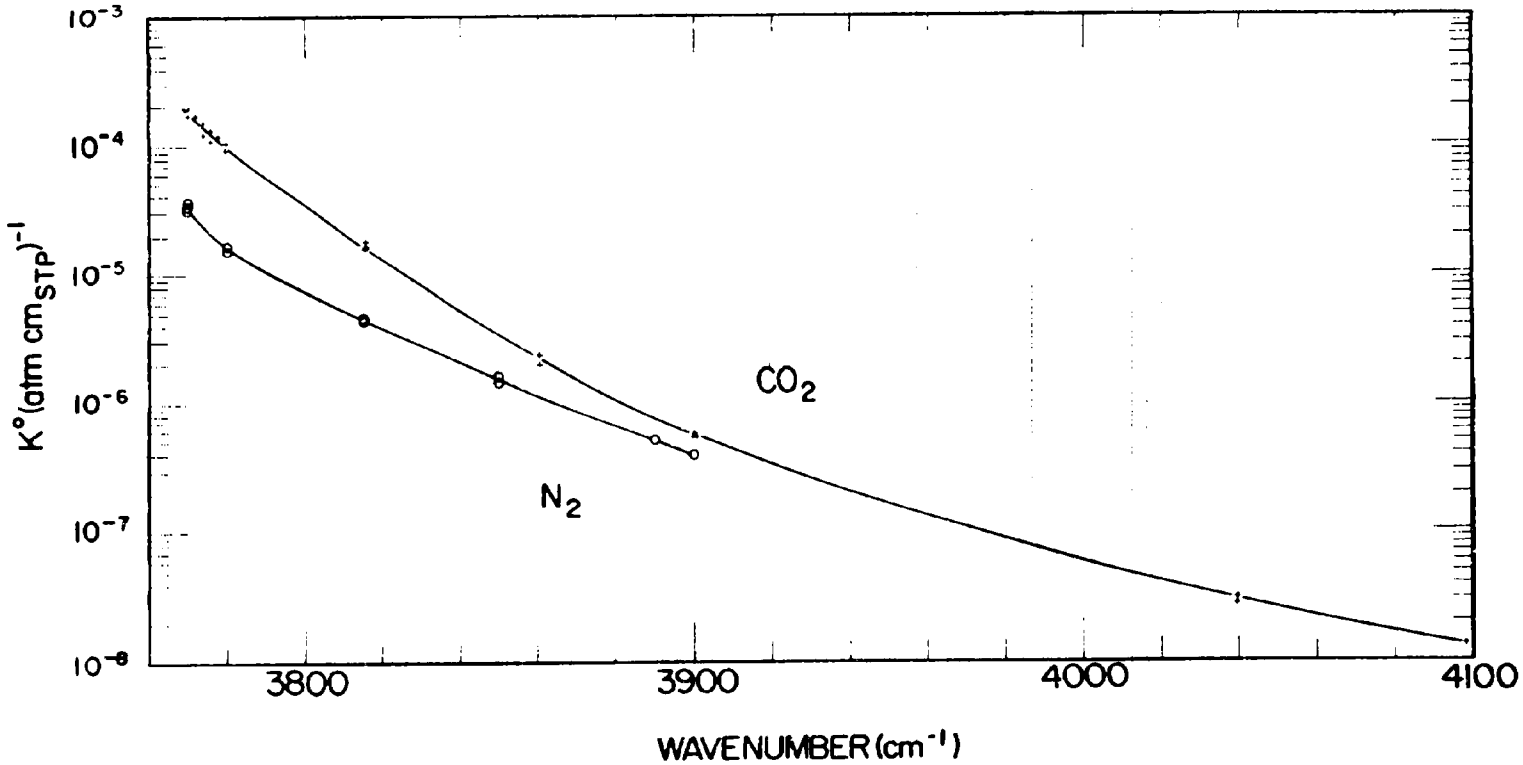

FIG. 4-1. ABSORPTION COEFFICIENT BETWEEN 3770 AND 4100 cm^{-1} DUE TO WINGS OF STRONG CO_2 LINES AT LOWER WAVENUMBERS.

The upper curve corresponds to self-broadening and the lower curve to N_2 broadening at 1 atm pressure.

SECTION 5

REFERENCES

1. D. E. Burch, D. A. Gryvnak, and Dudley Williams, Appl. Opt. 1, 759 (1962).

2. J. N. Howard, D. E. Burch, and Dudley Williams, J. Opt. Soc. Am. 46, 237 (1956).

3. D. E. Burch, D. A. Gryvnak, and R. R. Patty, Absorption by CO_2 Between 4500 and 5400 cm^{-1}, Aeronutronic Report U-2955, Contract NOnr 3560(00), 15 December 1966.

4. D. E. Burch, D. A. Gryvnak, and R. R. Patty, J. Opt. Soc. Am. 57, 885 (1967).

5. V. R. Stull, P. J. Wyatt, and G. N. Plass, The Infrared Absorption of Carbon Dioxide, Aeronutronic Report SSD-TDR-62-127, Contract AF19(604)-7479, 1963.

6. C. P. Courtoy, Annales de la Societe Scientifique de Bruxelles, Series 1, pp5-230, 27 March 1959.

7. E. K. Plyler, E. D. Tidwell, and W. S. Benedict, Opt. Soc. Am. 52, 1017 (1962).

8. W. S. Benedict, Johns Hopkins University (Private Communications).

9. D. E. Burch and D. A. Gryvnak, Strengths, Widths, and Shapes of the Lines of the 3 CO Band, Aeronutronic Report U-3972, Contract NOnr 3560(00), 10 March 1967. Also J. Chem. Phys. 47, 4930 (1967).

10. D. F. Eggers and B. L. Crawford, J. Chem. Phys 19, 1554 (1951).

11. D. E. Burch, D. A. Gryvnak, and R. R. Patty, Absorption by CO_2 Between 8000 and 10,000 cm^{-1} (1-1.25 Micron Region), Aeronutronic Report U-3200, Contract NOnr 3560(00), 6 August 1965.

12. D. E. Burch, D. A. Gryvnak, and R. R. Patty, Absorption by CO_2 Between 6600 and 7125 cm^{-1} (1.4 Micron Region), Aeronutronic Report U-3127, Contract NOnr 3560(00), 25 June 1965.

13. D. E. Burch, D. A. Gryvnak, and R. R. Patty, Absorption by H_2O Between 2800 and 4500 cm^{-1} (2.7 Micron Region), Aeronutronic Report U-3202, Contract NOnr 3560(00), 30 September 1965.

14. D. E. Burch, D. A. Gryvnak, R. R. Patty, and C. E. Bartky, The Shapes of Collision-Broadened CO_2 Absorption Lines, Aeronutronic Report U-3203, Contract NOnr 3560(00), (To Be Published).

UNCLASSIFIED
Security Classification

DOCUMENT CONTROL DATA - R&D

(Security classification of title, body of abstract and indexing annotation must be entered when the overall report is classified)

1. ORIGINATING ACTIVITY (Corporate author)
Applied Research Laboratories
Aeronutronic Division
Philco-Ford Corporation

2a. REPORT SECURITY CLASSIFICATION
Unclassified

2b. GROUP

3. REPORT TITLE
Absorption by CO_2 Between 3100 and 4100 cm^{-1} (2.44 - 3.22 Microns)

4. DESCRIPTIVE NOTES (Type of report and inclusive dates)
Scientific Report

5. AUTHOR(S) (Last name, first name, initial)
Burch, Darrell E.
Gryvnak, David A.
Patty, Richard R.

6. REPORT DATE
30 April 1968

7a. TOTAL NO OF PAGES
31

7b. NO OF REFS
14

8a. CONTRACT OR GRANT NO.
NOnr3560(00)

b. PROJECT NO
ARPA Order No. 237

c. Amendment #23/1/3/66

d.

9a. ORIGINATOR'S REPORT NUMBER(S)
U-4132

9b. OTHER REPORT NO(S) (Any other numbers that may be assigned this report)
None

10. AVAILABILITY/LIMITATION NOTICES

11. SUPPLEMENTARY NOTES

12. SPONSORING MILITARY ACTIVITY

13. ABSTRACT

The absorption by CO_2 between 3100 and 4100 cm^{-1} has been studied with a spectrometer whose spectral slitwidth was approximately one-half cm^{-1}. Spectral curves were obtained for 26 samples of CO_2 and $CO_2 + N_2$ with pressures as high as 14.6 atmospheres and with paths as long as 933 meters. Several absorption bands not observed previously in laboratory spectra have been identified and the strengths of several bands have been determined. Absorption between 3770 and 4100 cm^{-1} by the extreme wings of strong lines at lower wavenumbers has been investigated for self-broadened and N_2-broadened lines. Spectral curves and extensive tables of $\int_{\nu_1}^{\nu_2} A(\nu)d\nu$ have been included for most of the samples.

DD FORM 1 JAN 64 1473

UNCLASSIFIED
Security Classification

UNCLASSIFIED

Security Classification

14. KEY WORDS	LINK A ROLE	LINK A WT	LINK B ROLE	LINK B WT	LINK C ROLE	LINK C WT
CO_2						
Infrared						
Absorption						
Collision Broadening						
Line Shapes						
Band Strengths						

INSTRUCTIONS

1. ORIGINATING ACTIVITY: Enter the name and address of the contractor, subcontractor, grantee, Department of Defense activity or other organization *(corporate author)* issuing the report.

2a. REPORT SECURITY CLASSIFICATION: Enter the overall security classification of the report. Indicate whether "Restricted Data" is included. Marking is to be in accordance with appropriate security regulations.

2b. GROUP: Automatic downgrading is specified in DoD Directive 5200.10 and Armed Forces Industrial Manual. Enter the group number. Also, when applicable, show that optional markings have been used for Group 3 and Group 4 as authorized.

3. REPORT TITLE: Enter the complete report title in all capital letters. Titles in all cases should be unclassified. If a meaningful title cannot be selected without classification, show title classification in all capitals in parenthesis immediately following the title.

4. DESCRIPTIVE NOTES: If appropriate, enter the type of report, e.g., interim, progress, summary, annual, or final. Give the inclusive dates when a specific reporting period is covered.

5. AUTHOR(S): Enter the name(s) of author(s) as shown on or in the report. Enter last name, first name, middle initial. If military, show rank and branch of service. The name of the principal author is an absolute minimum requirement.

6. REPORT DATE: Enter the date of the report as day, month, year; or month, year. If more than one date appears on the report, use date of publication.

7a. TOTAL NUMBER OF PAGES: The total page count should follow normal pagination procedures, i.e., enter the number of pages containing information.

7b. NUMBER OF REFERENCES: Enter the total number of references cited in the report.

8a. CONTRACT OR GRANT NUMBER: If appropriate, enter the applicable number of the contract or grant under which the report was written.

8b, 8c, & 8d. PROJECT NUMBER: Enter the appropriate military department identification, such as project number, subproject number, system numbers, task number, etc.

9a. ORIGINATOR'S REPORT NUMBER(S): Enter the official report number by which the document will be identified and controlled by the originating activity. This number must be unique to this report.

9b. OTHER REPORT NUMBER(S): If the report has been assigned any other report numbers *(either by the originator or by the sponsor)*, also enter this number(s).

10. AVAILABILITY/LIMITATION NOTICES: Enter any limitations on further dissemination of the report, other than those imposed by security classification, using standard statements such as:

(1) "Qualified requesters may obtain copies of this report from DDC."

(2) "Foreign announcement and dissemination of this report by DDC is not authorized."

(3) "U. S. Government agencies may obtain copies of this report directly from DDC. Other qualified DDC users shall request through _____."

(4) "U. S. military agencies may obtain copies of this report directly from DDC. Other qualified users shall request through _____."

(5) "All distribution of this report is controlled. Qualified DDC users shall request through _____."

If the report has been furnished to the Office of Technical Services, Department of Commerce, for sale to the public, indicate this fact and enter the price, if known.

11. SUPPLEMENTARY NOTES: Use for additional explanatory notes.

12. SPONSORING MILITARY ACTIVITY: Enter the name of the departmental project office or laboratory sponsoring *(paying for)* the research and development. Include address.

13. ABSTRACT: Enter an abstract giving a brief and factual summary of the document indicative of the report, even though it may also appear elsewhere in the body of the technical report. If additional space is required, a continuation sheet shall be attached.

It is highly desirable that the abstract of classified reports be unclassified. Each paragraph of the abstract shall end with an indication of the military security classification of the information in the paragraph, represented as *(TS)*, *(S)*, *(C)*, or *(U)*.

There is no limitation on the length of the abstract. However, the suggested length is from 150 to 225 words.

14. KEY WORDS: Key words are technically meaningful terms or short phrases that characterize a report and may be used as index entries for cataloging the report. Key words must be selected so that no security classification is required. Identifiers, such as equipment model designation, trade name, military project code name, geographic location, may be used as key words but will be followed by an indication of technical context. The assignment of links, rules, and weights is optional.